Mechanistic Studies of the 1,4-Cis Polymerization of Butadiene According to the π-Allyl Insertion Mechanism. 1. Density Functional Study of the C−C Bond Formation Reaction in Cationic (η^3-Allyl)(η^2-/η^4-butadiene)nickel(II) Complexes $[Ni(C_3H_5)(C_4H_6)]^+$ and $[Ni(C_3H_5)(C_4H_6)(C_2H_4)]^+$

Sven Tobisch,*,† Horst Bögel,† and Rudolf Taube*,‡

Institute of Physical Chemistry and Institute of Inorganic Chemistry, Department of Chemistry, Martin Luther University of Halle, Geusaer Strasse, D-06217 Merseburg, Germany

Received January 22, 1996[⊗]

The 1,4-cis polymerization of butadiene according to the π-allyl insertion mechanism has been studied theoretically by density functional theory (DFT) for the ligand free cationic butenylnickel(II) complexes $[Ni(C_3H_5)(C_4H_6)]^+$, **I** and $[Ni(C_3H_5)(C_4H_6)(C_2H_4)]^+$, **II**. DFT energy profiles have been determined for the insertion of *s-cis*-butadiene into the (η^3-butenyl)nickel-(II) bond in the supine and prone orientations of the reacting ligands. The primary goal of this study aims to show that the insertion of *cis*-butadiene into the nickel(II)−allyl bond can occur within the π-coordination of the reacting parts which is characterized by an insertion barrier that should make the process feasible. Due to the lack of coordinative saturation of nickel(II) in the simpler model **I**, the insertion was calculated to be endothermic, and no clear difference between the supine/prone arrangements was apparent. The influence of the next double bond of the growing polymer chain for an adequate description of the geometrical aspects, as well as reliable energetics of the insertion, was demonstrated by **II**. The insertion was calculated to be exothermic by 11.6 kcal/mol for supine and 17.3 kcal/mol for prone, while the activation barrier was estimated to be 26.4 kcal/mol for supine and 3.9 kcal/mol for prone. Preference is given to the prone orientation in kinetic and in thermodynamic control.

Downloaded by CARLI CONSORTIUM on June 30, 2009
Published on August 6, 1996 on http://pubs.acs.org | doi: 10.1021/om960038d

Introduction

Stereospecific butadiene polymerization was discovered by Natta[1] almost 40 years ago using organometallic catalysts of the Ziegler-type. Approximately 10 years later, it became evident that during the butadiene polymerization reaction allyl transition metal complexes were the real catalytic species.[2]

It was recognized that the chain growth proceeds by the insertion of butadiene into the allyl transition metal bond. This was proved directly by following the polymerization reaction by NMR spectroscopy for the allylnickel iodide[3a] as a 1,4-trans and allylnickel trifluoroacetate[3b] as a 1,4-cis regulating catalyst.

The elucidation of the mechanism of stereoregulation proved to be a much more complicated task. The difficulties arose from the large number of different possibilities in structure and reactivity for the polybutadienyl group and the catalytically active transition metal complex. Therefore, four different modes of butadiene coordination (η^2-cis, η^2-trans, η^4-cis, η^4-trans) and two different structures of the η^3-coordinated butenyl end group (anti-η^3, syn-η^3) must be taken into account giving rise to eight structurally different catalyst complexes, all of which are capable of achieving the insertion step. All these catalyst complexes may be in equilibrium which could either be relatively slow or relatively rapid.

The insertion of butadiene into the allyl transition metal bond may occur according to two different mechanisms. Cossee and Arlman[4] first suggested that the η^2- or η^4-coordinated butadiene, when acting as an electrophile, could be nucleophilically attacked by the butenyl end group in its η^1-coordination. In contrast, to the σ-allyl insertion mechanism, the butenyl group may also react with butadiene in its η^3-state. This π-allyl insertion mechanism was introduced by Taube et al.[5a] in order to relate the cis−trans selectivity to the reactivity of the butenyl group in its anti or syn configuration.[5] The way in which the two mechanisms are achieved depends on the balance between the need of energy for structure variation and the gain in energy from stronger interaction between the reactants in the coordination sphere of the metal atom.

† Institute of Physical Chemistry,
‡ Institute of Inorganic Chemistry.
[⊗] Abstract published in *Advance ACS Abstracts,* July 1, 1996.

(1) Natta, G. *Angew. Chem.* **1956**, *68*, 393.
(2) (a) Porri, L.; Natta, G.; Gallazzi, M. C. *Chim. Ind.* **1964**, *46*, 2525. (b) Porri, L.; Natta, G.; Gallazzi, M. C. *J. Polym. Sci. C* **1967**, *16*, 2525. (c) Babitskii, B. D.; Dolgoplosk, B. A.; Kormer, V. A.; Lobach, M. I.; Tinakova, E. I.; Yakovlev, V. A. *Isv. Akad. Nauk SSSR Ser. Chem.* **1965**, 1507. (d) Wilke, G.; et al. *Angew. Chem.* **1966**, *78*, 157.
(3) (a) Lobach, M. I.; Kormer, V. A.; Tsereteli, I. Yu.; Kondoratenkov, G. P.; Babitskii, B. D.; Klepikova, V. I. *J. Polym. Sci., Polym. Lett.* **1971**, *9*, 71. (b) Warin, R.; Teyssie, Ph.; Bourdaudurq, P.; Dawans, F. *J. Polym. Sci.,* Polym. *Lett.* **1973**, *11*, 177.
(4) (a) Cossee, P. In *Stereochemistry of Macromolecules*; Ketley, A. D., Ed.; Marcel Dekker Inc.: New York, 1967; Vol. 1, p 145. (b) Arlman, E. J. *J. Catal.* **1966**, *5* 178.
(5) (a) Taube, R.; Gehrke, J.-P.; Radeglia, R. *J. Organomet. Chem.* **1985**, *291*, 101. (b) Taube, R.; Gehrke, J.-P.; Böhme, P. *Wiss. Z. TH Leuna-Merseburg* **1987**, *39*, 310. (c) Sieler, J.; Kempe, R.; Wache, S.; Taube, R. *J. Organomet. Chem.* **1993**, *455*, 241. (d) Taube, R.; Wahe, S.; Sieler, J.; Kempe, R. *J. Organomet. Chem.* **1993**, *456*, 131. (e) Taube, R.; Schmidt, U.; Gehrke, J.-P.; Böhme, P.; Langlotz, J.; Wache, S. *Makromol. Chem., Macromol. Symp.* **1993**, *66*, 245. (f) Taube, R.; Windisch, H.; Maiwald, S. *Makromol. Chem., Macromol. Symp.* **1995**, *89*, 393.

S0276-7333(96)00038-6 CCC: $12.00 © 1996 American Chemical Society

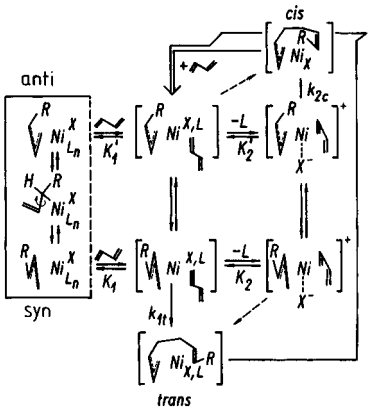

Figure 1. General mechanistic scheme for the catalysis of the cis and trans 1,4-polymerization of butadiene by allylnickel(II) complexes. For a detailed analysis, see Taube et al.[5]

According to the principle of least structure variation, it is expected that, in the 1,4-polymerization, the insertion reaction with the η^4- or η^2-coordinated butadiene in the single cis configuration will lead to an anti structure of the butenyl end group (anti insertion), while the butadiene coordination in the single trans configuration will give rise to a syn structure (syn insertion). Furthermore, the cis and trans configurations of the double bond in the new C_4 unit will be determined by the anti or syn configuration of the reacting butenyl group.

With the synthesis and characterization of the cationic (C_{12}-allyl)nickel(II) complex $[Ni(C_{12}H_{19})][B(C_6H_3(CF_3)_2)_4]$, Taube et al.[6] have proved conclusively that the cationic (polybutadienyl)(butadiene)nickel(II) complex $[RC_3H_4Ni(C_4H_6)]^+$ is the real catalyst for the 1,4-cis polymerization of butadiene. A general mechanistic scheme for both the catalysis of the cis and trans 1,4-polymerization of butadiene by allylnickel(II) complexes is outlined in Figure 1. Accordingly, the cis−trans selectivity is not determined by the rate of anti−syn isomerization, as suggested in the literature,[7] but by the different reactivity of the *anti*- and the *syn*-butenylnickel(II) complexes with respect to the mode of butadiene coordination. This can be explained by the different steric hindrance during the formation of the transition state of the insertion reaction. In the monoligand butenylnickel(II) complex with η^2-coordinated butadiene the C−C bond formation is less hindered sterically if the growing chain is arranged in the syn position. Therefore, the formation of trans units is catalyzed via the reaction channel k_{1t}.[5c] In the ligand-free cationic butenylnickel(II) complex, the insertion step can only take place via the coordinative interaction of the next double bond to the nickel center, in order to stabilize the transition state in compliance with Tolman's 18−16-electron rule. In this case, the anti complex becomes more reactive than the syn complex and a cis unit can be easily generated with the η^4-cis-coordinated butadiene in a "prone" arrangement, according to the reaction channel k_{2c}.[5d]

As far as we know, up to now no theoretical study has been carried out concerning the π-allyl insertion mechanism by means of reliable ab initio methods. The here presented results were obtained by utilizing a density functional theory (DFT) based method. A number of recent studies have evaluated DFT as a practical tool for the reliable estimation of geometrical, as well as energetic properites, for a wide range of different molecular systems.[8] The usual trend indicates that the current approximate gradient functionals provide more accurate results than the simple local density approximation (LDA) based DFT method. This is especially remarkable for transition metal complexes,[9] bearing in mind the great difficulties of the traditional HF-based methods and the partly enormous computational effort of correlated methods needed to overcome this. In a former study the reliability of the DFT method was proved by the remarkably good agreement between the calculated equilibrium geometries and relative energies and the experimental knowledge with regards to the accessible key structures of the mechanism.[10]

As the first part of a series of papers, we will present our results for the *s-cis*-butadiene insertion into the η^3-butenyl−nickel(II) bond which generates a new cis-C_4 unit. The investigations were carried out on two systems modeling the ligand−free cationic butenylnickel(II) complex: first on the allyl(butadiene)nickel(II) $[Ni(C_3H_5)(C_4H_6)]^+$ complex and second on the same complex including an additional ethylene ligand, $[Ni(C_3H_5)(C_4H_6)(C_2H_4)]^+$, which represents the next double bond of the growing polymer chain. The effect of the counterion or solvent in the catalytic process was neglected in consideration of the present computational resources available.

As our primary aim, we will show that the butadiene insertion into the nickel−allyl bond can occur within π-coordination with a barrier, which indicates that this process is feasible. The second objective is related to the stabilizing effect of the next double bond to the nickel center and the need to obtain a correct picture of the π-insertion reaction.

Computational Details

The approximate density functional calculations reported here were performed by using the DGauss program within the UniChem software environment.[11]

All calculations were carried out using the LDA with Slater's exchange functional[12a,b] and Vosko−Wilk−Nusair parametrization on the homogeneous electron gas for correlation,[12c] augmented by gradient corrections to the exchange-correlation

(6) (a) Taube, R.; Wache, S. *J. Organomet. Chem.* **1992**, *428*, 431. (b) Wache, S.; Taube, R. *J. Organomet. Chem.* **1993**, *456*, 137.

(7) (a) Jolly, P. W.; Wilke, G. *The Organic Chemistry of Nickel, Vol. 2, Organic Synthesis*; Academic Press: New York, 1975, p 225. (b) Dolgoplosk, B. A. *Sov. Sci. Rev. Sect. B* **1980**, *2*, 203.

(8) (a) Andzelm, J.; Wimmer, E. *J. Chem. Phys.* **1992**, *96*, 1280. (b) Becke, A. D. *J. Chem. Phys.* **1992**, *96*, 2155. (c) Johnson, B. G.; Gill, P. M. W.; Pople, J. A. *J. Chem. Phys.* **1993**, *98*, 5612. (d) Gill, P. M. W.; Johnson, B. G.; Pople, J. A.; Frisch, M. A. *Int. J. Quant. Chem., Quant. Chem. Symp.* **1992**, *26*, 319. (e) Ziegler, T. *Chem. Rev.* **1991**, *91*, 651. (f) Ziegler, T. *Can. J. Chem.* **1995**, *73*, 743. (g) Jones, R. O.; Gunnarsson, O. *Rev. Mod. Phys.* **1989**, *61*, 689. (h) Oliphant, N.; Bartlett, R. J. *J. Chem. Phys.* **1994**, *100*, 6550.

(9) (a) Fan, L.; Ziegler, T. *J. Chem. Phys.* **1991**, *95*, 7401. (b) Scuseria, G. E. *J. Chem. Phys.* **1992**, *97*, 7528. (c) Eriksson, L. A.; Pettersson, L. G. M.; Siegbahn, P. E. M.; Wahlgren, U. *J. Chem. Phys.* **1995**, *102*, 872.

(10) Tobisch, S.; Bögel, H.; Taube, R. Manuscript in preparation.

(11) (a) Andzelm, J.; Wimmer, E. *Physica B* **1991**, *172*, 307. (b) Andzelm, J. In *Density Functional Methods in Chemistry*; Labanowski, J.; Andzelm, J., Eds.; Springer: Berlin, 1991. DGauss and UniChem are software packages available from Cray Research.

(12) (a) Dirac, P. A. M. *Proc. Cambridge Philos, Soc.* **1930**, *26*, 376. (b) Slater, J. C. *Phys. Rev.* **1951**, *81*, 385. (c) Vosko, S. H.; Wilk, L.; Nusair, M. *Can. J. Phys.* **1980**, *58*, 1200. (d) Becke, A. D. *Phys. Rev.* **1988**, *A38*, 3098. (e) Perdew, J. P. *Phys. Rev.* **1986**, *B33*, 8822.

Downloaded by CARLI CONSORTIUM on June 30, 2009
Published on August 6, 1996 on http://pubs.acs.org | doi: 10.1021/om960038d

potential. Gradient corrections for exchange based on the functional of Becke[12d] and for correlation based on Perdew[12e] were added variationally within the SCF procedure (LDA/BP-NLSCF).

All-electron Gaussian orbital basis sets were used for all atoms. The calculations were performed with two different basis sets, denoted DZVP and TZVP. Our standard DZVP basis is a 15s/9p/5d set contracted to (63321/531/41) for nickel,[13a] a 9s/5p/1d set contracted to (621/41/1) for carbon,[13b] and a 4s/1p set contracted to (31/1) for hydrogen.[13b] Corresponding auxiliary basis sets were used for the fitting of the charge density.[13b] The TZVP basis set consisted of orbital functions with the contraction patterns (63321/5211/41), (7111/411/1), and (311/1) for Ni,[13a] C,[13b] and H,[13b] respectively.

The numerical integration was done by using a standard fine meshed grid of adequate quality. The effect of tighter meshed grids was evaluated to be not more than 0.2 kcal/mol for total energies, as indicated by single point calculations with more than twice as many integration points as in our standard fine grid.

The geometry optimization and the saddle point search were performed at the LDA/BP-NLSCF level of approximation by utilizing analytical gradients/hessians according to standard algorithms. No symmetry constraints were imposed in any optimization. The stationary points were identified exactly by the curvature of the potential surface at these points corresponding to the eigenvalues of the analytically calculated hessian.

Results and Discussion

We shall here present the results gained from our DFT calculations on the cationic $[Ni(C_3H_5)(C_4H_6)]^+$ and $[Ni(C_3H_5)(C_4H_6)(C_2H_4)]^+$ complexes, which were chosen as minimal models of the real active catalyst, the cationic (polybutadienyl)(butadiene)nickel(II) complex $[RC_3H_4Ni(C_4H_6)]^+$. The structures of the butadiene-coordinated educts were derived from introductory investigations of the anti/syn η^3-butenyl coordination on the cationic (C_{12}-allyl)nickel(II) complex.[14] In each of the two model systems, both the "supine" (i.e. the reacting η^2-/η^4-butadiene and η^3-butenyl group are oriented as back to back) and the "prone" (i.e. the reacting η^2-/η^4-butadiene and η^3-butenyl group are oriented as back to stomach) arrangements have been investigated.[15]

We do not expect to find large differences in the smaller $[Ni(C_3H_5)(C_4H_6)]^+$ complex between the educts, products, and transition states in supine and prone arrangements, respectively, due to the lack of coordinative saturation of nickel(II).

In the more realistic $[Ni(C_3H_5)(C_4H_6)(C_2H_4)]^+$ complex, concerning the educts the ethylene ligand is oriented above the nickel(II) coordination plane, modeling the orientation of the next double bond in the growing polymer chain in the case of an anti η^3-butenyl group. Here it is important to see how this additional double bond can stabilize the transition state of the supine and prone configurations in different ways.

We shall start with a comparison of the π-allyl insertion on the $[Ni(C_3H_5)(C_4H_6)]^+$-based system. The discussion will be followed by an examination of the $[Ni(C_3H_5)(C_4H_6)(C_2H_4)]^+$-based systems and a detailed investigation of the role of the additional double bond.

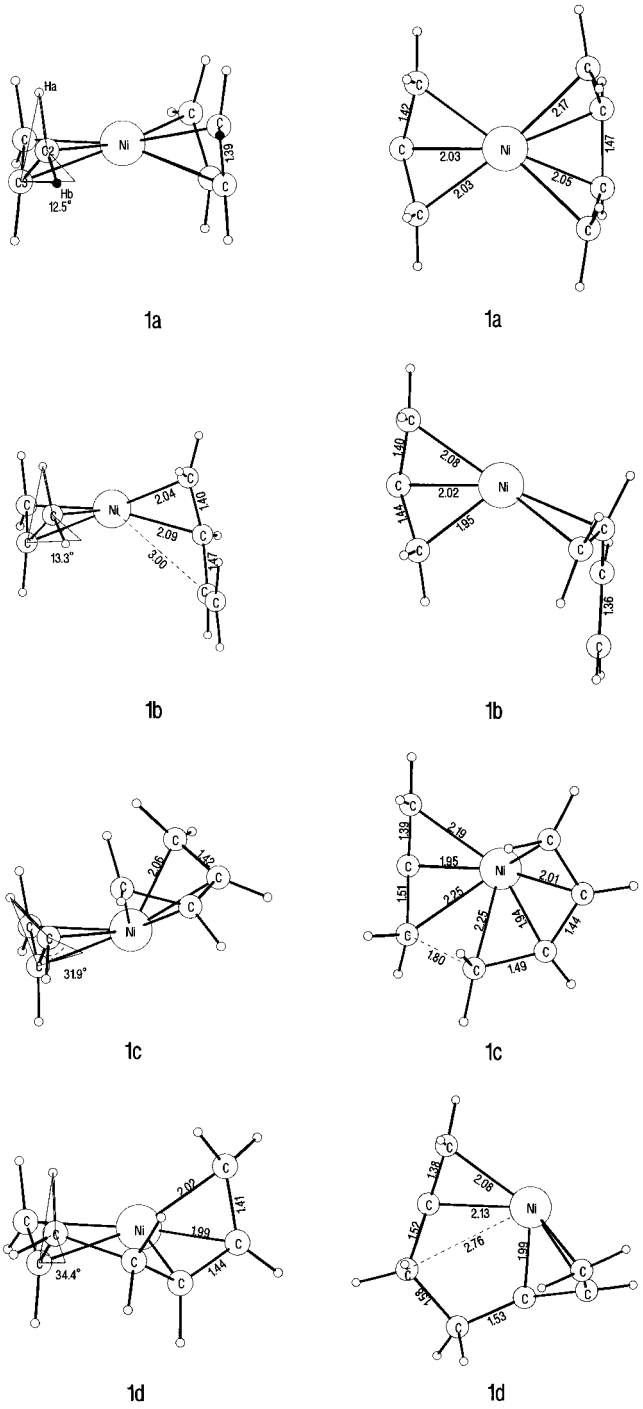

Figure 2. Optimized structures for the η^4-/η^2-butadiene educts **1a**/**1b**, the transition state **1c**, and the product **1d** of the supine $[Ni(C_3H_5)(C_4H_6)]^+$ complex (bond lengths in Å and angles in deg).

Cationic $[Ni(C_3H_5)(C_4H_6)]^+$ Complex. The optimized structures of the η^4-butadiene educts (**1a**, **2a**), the η^2-butadiene educts (**1b**, **2b**), the transition states (**1c**, **2c**), and the products (**1d**, **2d**) for the supine/prone arrangements are shown in Figures 2 and 3, respectively, where they are depicted in two different views: first, the square-planar nickel(II) coordination plane formed by nickel and the two terminal carbon atoms of the reacting allylic part and, second, its perpendicular view. The prone product (**2d**) as an exception is displayed first with the terminal bond of the reacting allylic part perpendicular to the nickel plane and the corresponding perpendicular view. All optimized struc-

(13) (a) DGauss basis set library. (b) Godbout, N.; Salahub, D. R.; Andzelm, J.; Wimmer, E. *Can. J. Chem.* **1992**, *70*, 560.
(14) Tobisch, S. Unpublished data.
(15) Yasuda, H.; Nakamura, A. *Angew. Chem.* **1987**, *99*, 745.

Downloaded by CARLI CONSORTIUM on June 30, 2009
Published on August 6, 1996 on http://pubs.acs.org | doi: 10.1021/om960038d

Downloaded by CARLI CONSORTIUM on June 30, 2009
Published on August 6, 1996 on http://pubs.acs.org | doi: 10.1021/om960038d

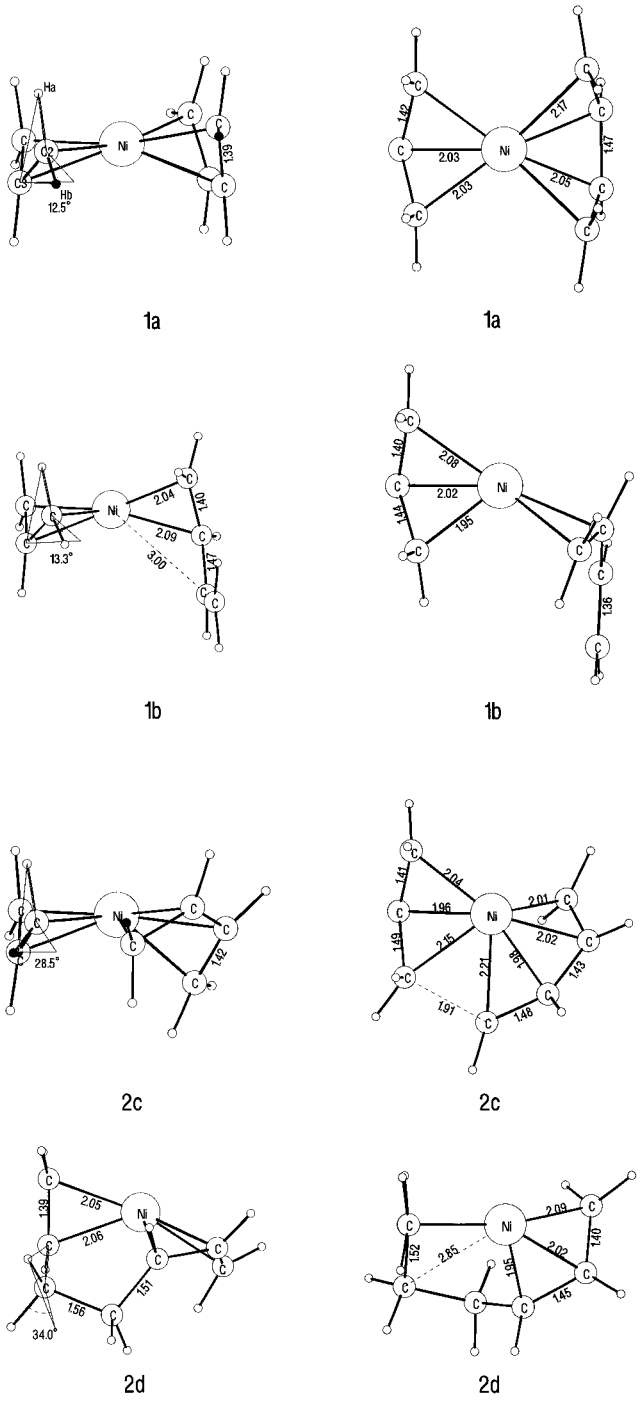

Figure 3. Optimized structures for the η^4-/η^2-butadiene educts **2a**/**2b**, the transition state **2c**, and the product **2d** of the prone $[Ni(C_3H_5)(C_4H_6)]^+$ complex (bond lengths in Å and angles in deg).

tures have C_1 symmetry, apart from the η^4-butadiene educts (**1a**, **2a**) which possess C_s symmetry.

As expected for all optimized structures, no clear differences for the main geometrical parameters between the supine and prone coordination are detected.

In the first step butadiene binds to the positively charged metal center forming stable educts in the preferred η^4-mode. The bonding in these complexes arise mainly from the interaction of the highest occupied π orbitals of allyl and butadiene with the formally vacant d_{xy} Ni(II) orbital (lying in the square planar complex plane), which gives rise to a bonding (**1a-I**, **2a-I**) and antibonding (**1a-II**, **2a-II**) combination (Figure 4). As indicated by **1a-II** and **2a-II**, the Ni(II) d_{xy} orbital tends to delocalize back from the terminal carbons of butadiene (where the 2π orbital is mainly located) in order to avoid the repulsive interaction. Additionally, the ligands move to a certain degree from the square planar coordination plane, which on the other hand may reduce the bonding interaction in **1a-I** and **2a-I**. Concerning the prone orientation the repulsive interaction should better be avoided by simultaneously retaining a stronger bonding interaction than in the supine orientation, as indicated by the fact that **2a** is more stable than **1a** by about 7 kcal/mol.

The nickel(II)−allyl coordination in the η^4-educts (**1a**, **2a**) is comparable to the bis(η^3-allyl)nickel(II) complex.[16] The nickel−carbon distances are similar, whereas the elongation of the allylic bond by 0.01 Å is somewhat smaller. The butadiene double bonds are elongated by 0.039 Å with regard to the uncoordinated butadiene. The quasi square-planar nickel(II) coordination plane is spread out by the terminal allylic and butadiene carbon atoms, according to the nodal structure of the HOMO of both ligands. In **1b** and **2b** the η^2-butadiene is not coordinated in a quasi planar manner. Even though the η^2-butadiene double bond and the allylic system are elongated to the same extent as in **1a** and **2a** (however unsymmetrical), the uncoordinated butadiene double bond remains unchanged; thus the η^2-butadiene appears as vinylethene.

In the second step the butadiene inserts into the nickel(II)−allylic bond to form the transition states **1c** and **2c**. As a result of the C−C σ-bond formation, a η^2-double bond in the growing chain and a new η^3-allylic system are generated in the products **1d** and **2d**; therefore, the products **1d** and **2d** resemble the educt structures. A new η^3-allylic moiety is formed to which the next butadiene can insert in order to propagate the polymerization further. Whereas the σ-bond is not directly involved in the nickel(II) coordination sphere, the η^2-double bond and the η^3-allylic system are still retained in π-coordination. Additionally, it is remarkable to notice that the coordination of the π-moieties occurs to nearly the same extent as in **1b** and **2b**.

The product structures are already preformed in the transition states **1c** and **2c**. Both the new η^3-allylic system, in the inserting butadiene, as well as the terminal η^2-double bond, in the former allylic part, are clearly generated. Furthermore, the adjacent bonds of the C−C σ-bond (in the process of being formed) are elongated to a considerable extend to form single bonds. In the transition states the reaction centers for the C−C bond formation are at distances of 1.796 Å (**1c**) and 1.909 Å (**2c**). These rather small distances are directly related to the lower coordination number of the nickel(II) center. A clear indication for the progress of the C−C σ-bond formation may be derived from the out of plane bending angle[17] $H_bC_3H_aC_2$, as displayed in Figures 2 and 3. This value can be used as a measure of the change in hybridization during the insertion process, which changes from approximately 12° for the educts to 34° for the products. The values of approximately 32 and 28° for **1c** and **2c**, respectively, point to a large change in hybridization from sp^2 to sp^3 at the transition

(16) Tobisch, S.; Boegel, H. *Int. J. Quant. Chem.* **1995**, *56*, 575.
(17) For an ideal sp^2/sp^3 hybridization, values of 0°/35.3° are expected.

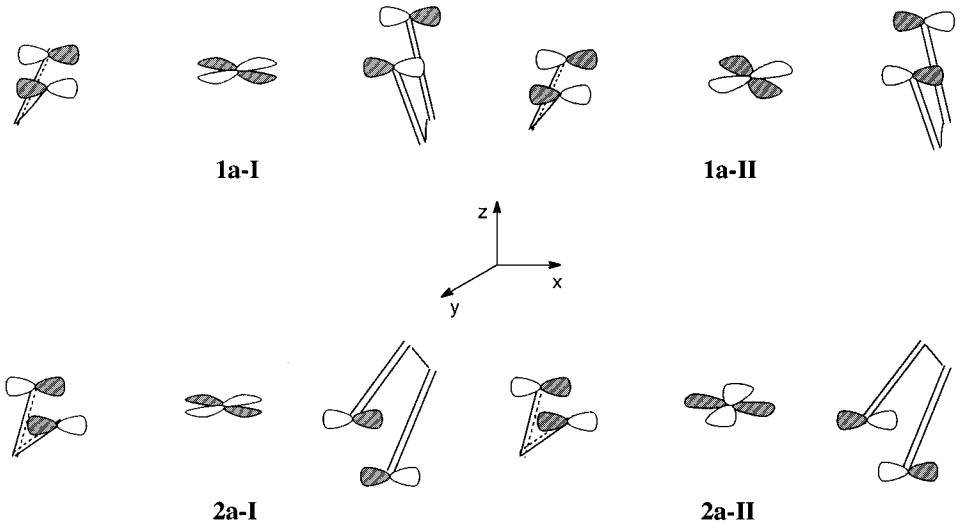

Figure 4.

Table 1. Calculated Energy Profile for the π-Allyl Insertion into the Cationic $[Ni(C_3H_5)(C_4H_6)]^+$ System (kcal/mol)[a]

system	η^4-educt (**1a**/**2a**)	η^2-educt (**1b**/**2b**)	transn state (**1c**/**2c**)	product (**1d**/**2d**)
supine (**1a**−**d**)	65.0	47.3	41.0	58.0
prone (**2a**−**d**)	71.9	46.4	46.4	63.3

[a] The isolated reactants ($[Ni(\eta^3\text{-}C_3H_5)]^+$ and *s-cis*-C_4H_6) were chosen as reference points.

state. As a consequence, the two sp^3-like carbon atoms (preformed for joining the C−C σ-bond) begin to move away from the nickel(II) coordination sphere, while the other parts remain in π-coordination to nickel(II). Therefore the transition states give a clear indication toward the π-insertion mechanism. Although the geometry of the transition states are comparable (as pointed out in Figures 2 and 3), **1c** appears more productlike than **2c**.

In optimizations starting from small distorted transition state geometries in the direction of educts and products, respectively, it was proved that both transition states correspond to both the η^4-butadiene educts (**1a**, **2a**) and the appropriate products (**1d**, **2d**). This agrees with the assumptions made according to the principle of least structure variation, which states the η^2-butadiene educts (**1b**, **2b**) should only be transient forms during the process of forming η^4-butadiene educts (**1a**, **2a**).

Table 1 shows the calculated energy profile by using the standard DZVP basis. Similar to the geometrical structure, no clear differences between the supine and prone coordinations could be detected. The η^4-educts (**1a**, **2a**) are formed in an exothermic reaction which are 65.0 and 71.9 kcal/mol, respectively, more stable than the isolated molecules. The overall reaction is exothermic by 58.0 kcal/mol (supine) and 65.3 kcal/mol (prone), but in contrast to the experimental findings, the insertion reaction (relative to the η^4-educts) was calculated endothermic by about 7 kcal/mol in both arrangements, which is understandable in relation to the rather crude reaction model. Whereas 16 electrons are involved in the coordinative interaction in the η^4-butadiene educts (**1a**, **2a**), all other systems are characterized by only 14 electrons; thus Tolman's 18−16 electron rule cannot be fulfilled and the extra stabilizing of the η^4-butadiene educts (**1a**, **2a**) is obvious. Additionally, due to the lack of coordinative saturation of the nickel(II) center, quite similar activation barriers of 24.0 and 25.5 kcal/mol for the supine and prone orientations, respectively, were calculated, to be higher than expected from polymerization experiments.

An indication of the standard DZVP basis's reliability is given by single point calculations with the larger TZVP basis. The relative changes in energetics are sufficiently small, about 1 kcal/mol for the supine and up to 4 kcal/mol for the prone arrangement.

To conclude, the cationic $[Ni(C_3H_5)(C_4H_6)]^+$ model allows a first insight into mechanistic aspects of the π-allyl insertion reaction. In the transition states, the process of forming the new C−C σ-bond can clearly be observed while the reacting moieties retained π-coordination. In accordance with the principle of least structure variation the η^2-butadiene educts (**1b**, **2b**) should only be transient forms when forming the η^4-butadiene educts (**1a**, **2a**). As expected, no clear kinetic or thermodynamic preference of the supine or prone orientation could be detected, although the prone structures (**2a**,**c**,**d**) are stabilized relative to the supine structures (**1a**,**c**,**d**). The endothermicity of the insertion reaction and the relatively high calculated activation barriers are clearly related to the low coordination number of the nickel(II) center. Therefore a reliable description of the reaction profile for this process is prevented because of the lack of coordination saturation of the nickel(II) center.

Cationic $[Ni(C_3H_5)(C_4H_6)(C_2H_4)]^+$ Complex. The optimized structures of the η^4-butadiene educts (**3a**, **4a**), the η^2-butadiene educts (**3b**, **4b**), the transition states (**3c**, **4c**), and the products (**3d**, **4d**) for the supine/prone arrangements are shown in Figures 5 and 6, respectively. They are depicted in the same manner as described in the previous section. All optimized structures have C_1 symmetry.

Under the influence of the next double bond of the growing polymer chain, modeled by the additional ethylene ligand, there is a different ligand coordination for the η^4-butadiene educts (**3a**, **4a**). To illustrate this, η^4-educt structures similar to **1a** and **2a** are investigated under the assumption of C_s symmetry with an additional ethylene ligand in the *z*-position (Figure 7). As a result of the additional double bond, the allylic and

Downloaded by CARLI CONSORTIUM on June 30, 2009
Published on August 6, 1996 on http://pubs.acs.org | doi: 10.1021/om960038d

Downloaded by CARLI CONSORTIUM on June 30, 2009
Published on August 6, 1996 on http://pubs.acs.org | doi: 10.1021/om960038d

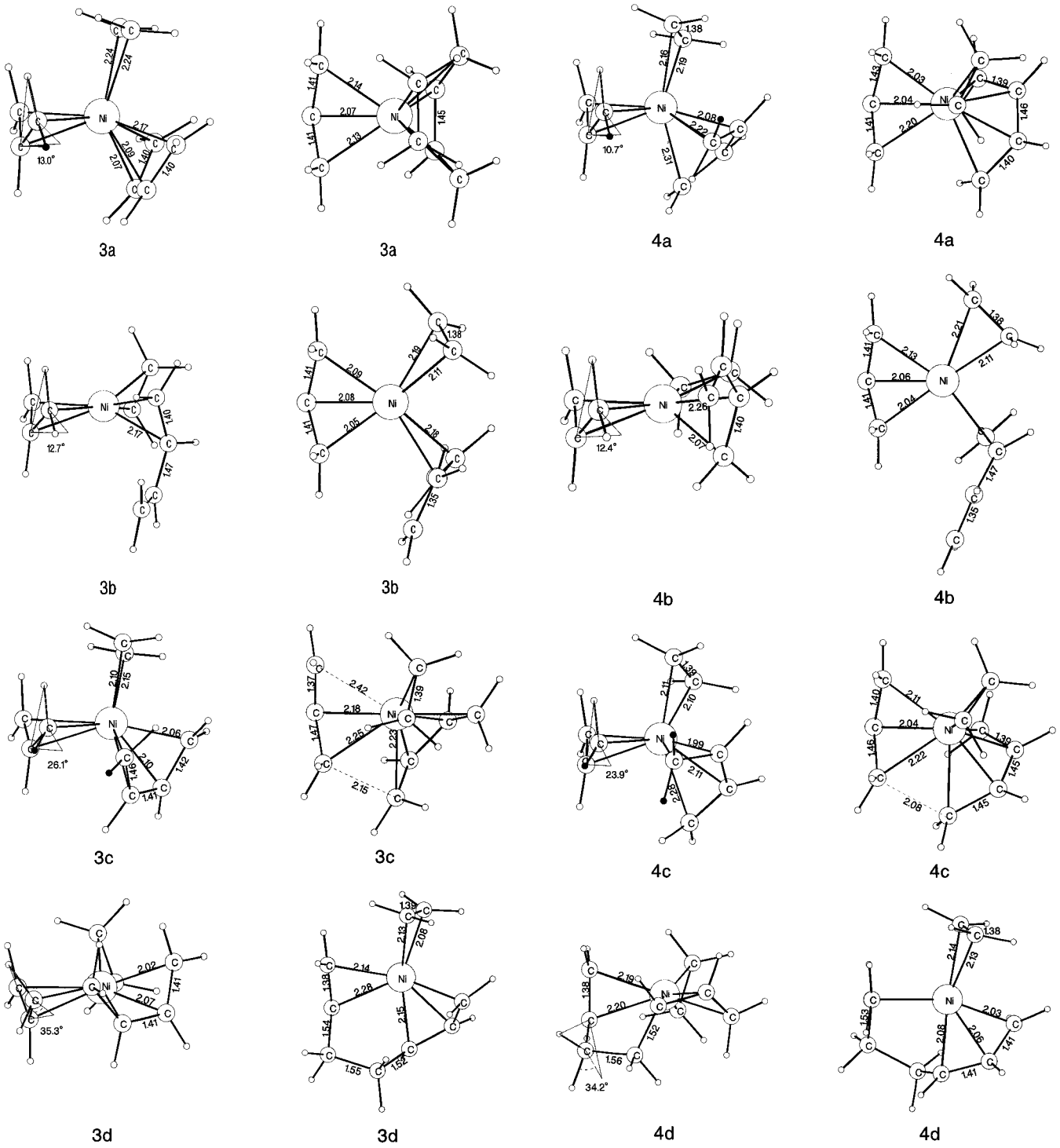

Figure 5. Optimized structures for the η^4-/η^2-butadiene educts **3a**/**3b**, the transition state **3c**, and the product **3d** of the supine $[Ni(C_3H_5)(C_4H_6)(C_2H_4)]^+$ complex (bond lengths in Å and angles in deg).

Figure 6. Optimized structures for the η^4-/η^2-butadiene educts **4a**/**4b**, the transition state **4c**, and the product **4d** of the prone $[Ni(C_3H_5)(C_4H_6)(C_2H_4)]^+$ complex (bond lengths in Å and angles in deg).

butadiene parts have to move from the quasi planar nickel(II) coordination plane. The nature of bonding of the ligands is quite similar to that in **1a** and **2a**, a bonding interaction with the formally vacant Ni(II) d_{xy} orbital (**3A-I**, **4A-I**) and a repulsive interaction with a metal orbital (a d_{yz}/p_y hybrid) which is mainly delocalized back from the terminal butadiene carbons. Additionally a high−lying occupied orbital is displayed (**3A-III**, **4A-III**), which essentially shows the repulsive interaction between the metal d_{z^2} orbital and the ethylene π-orbital (Figure 8). The supine structure **3A** is about 5 kcal/mol more stable than the prone structure **4A**, in contrast to the order of stability which has been found for **1a** and **2a**. The different stability is understandable in relation to the different extent of interaction of the HOMO of allyl and butadiene with appropriate metal d orbitals.

Besides the quadratic pyramidal ligand orientation, there is also an trigonal bipyramidal orientation, which is favored by energy. The quasi trigonal bipyramidal prone η^4-educt **4a** is about 2 kcal/mol more stable than the corresponding quadratic pyramidal structure **4A**.

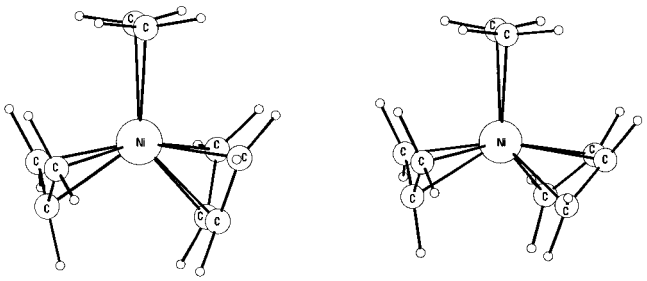

Figure 7. C_s-symmetrical model η^4-butadiene educt structures **3A/4A**.

This gain in energy may mainly be attributed to the effective interaction of butadiene with the d_{z^2} metal AO (**4a-III**) (Figure 9). Therefore, an additional π-coordinated double bond in the *z*-position relative to the quasi planar nickel(II) coordination plane leads to a different ligand coordination for the supine and prone orientations.

In the supine η^4-educt (**3a**), which is nearly identical to **3A**, the nickel(II)−allyl and nickel(II)−butadiene distances are elongated as compared to **1a**. The butadiene ligand is somewhat more, by about 0.048 Å for the double bond, and the allyl ligand somewhat less, by about 0.005 Å, distorted than in **1a**. As indicated by the extent of distortion of the carbon framework, a tighter coordination of the ethylene and ally ligands as well as a weaker coordination of butadiene than in **3a** is found in the prone η^4-educt (**4a**).

On the other hand quite similar changes in the ligand geometries occur concerning the η^2-educts (**3b**, **4b**); i.e., the additional ethylene does not cause large differences between the supine and prone coordination modes. The π-coordinated double bond of butadiene is distorted to the same extent as in **3a** and **4a**, while the uncoordinated butadiene double bond remains unchanged, and thus, the η^2-butadiene appears as vinylethene. In order to maintain the quasi planar nickel(II) coordination, the free movable ethylene ligand has been placed nearly perpendicular to the nickel(II) plane.

The products (**3d**, **4d**) are characterized by the newly formed C−C σ-bond, which is not directly involved in the nickel(II) coordination sphere, a π-coordinated cisoide η^2-double bond at the growing end, and a π-coordinated η^3-allylic part at the reactive end. The products (**3d**, **4d**) resemble the η^4-educts (**3a**, **4a**) as indicated by similar coordination of the π-moieties. To propagate the polymerization further, the next butadiene must replace the last π-coordinated double bond of the growing polymer chain, except for the next double bond to the reactive end, which forms a new educt structure. As a result of this, the butadiene can insert into the nickel(II)−allyl bond within the π-coordination generating a new cisoide C_4 unit.

The most remarkable differences in the geometrical structure and the energetics occur between the supine and prone orientations in the transition states (**3c**, **4c**). As for the corresponding η^4-educts, the supine transition state (**3c**) can be described as a tetragonal pyramid and the prone complex (**4c**) as a trigonal bipyramid. In the transition states, the reactive terminal allylic and butadiene carbon atoms are at distances of 2.155 Å (**3c**) and 2.079 Å (**4c**), which are noticeably larger than in **1c** and **2c**, indicating an earlier occurrence at the potential surfaces. Figures 5 and 6 show that, by means of the different extent of the distortion concerning the butadiene and allylic moieties, **3c** appears productlike whereas **4c** appears eductlike. Therefore, both the η^3-allylic part at the reactive end and the η^1-double bond at the growing chain are clearly preformed at this stage of the reaction for the supine coordination, both of them retained in π-coordination. On the other hand, in **4c** though the bonds adjacent to the C−C σ-bond (in the process of being formed) are considerably elongated, both ligands remain essentially in η^3-/η^4-π-coordination.

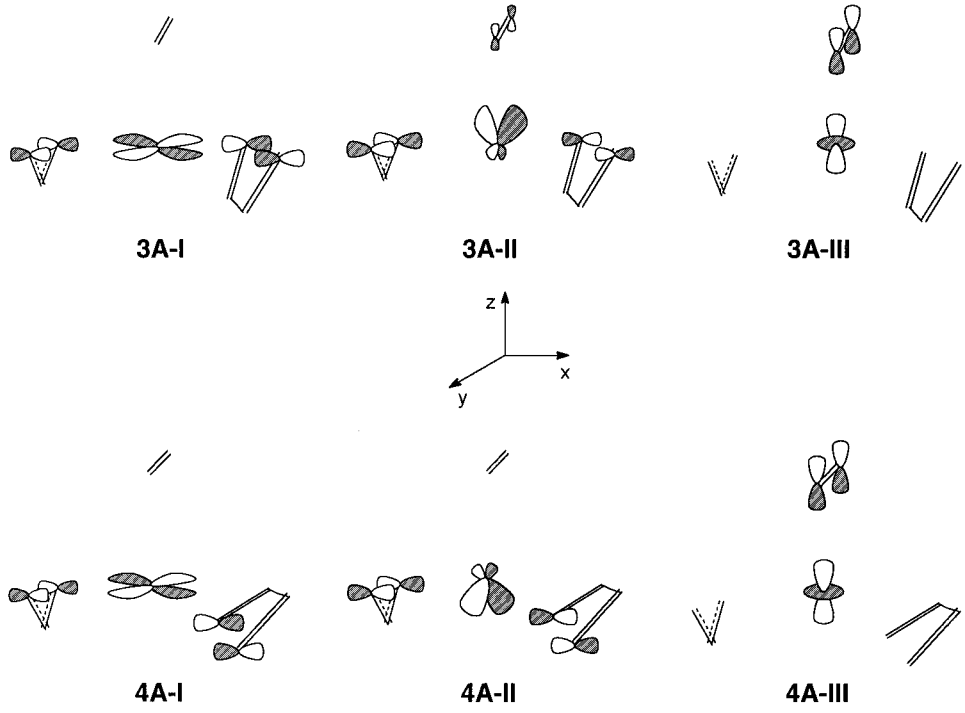

Figure 8.

Downloaded by CARLI CONSORTIUM on June 30, 2009
Published on August 6, 1996 on http://pubs.acs.org | doi: 10.1021/om960038d

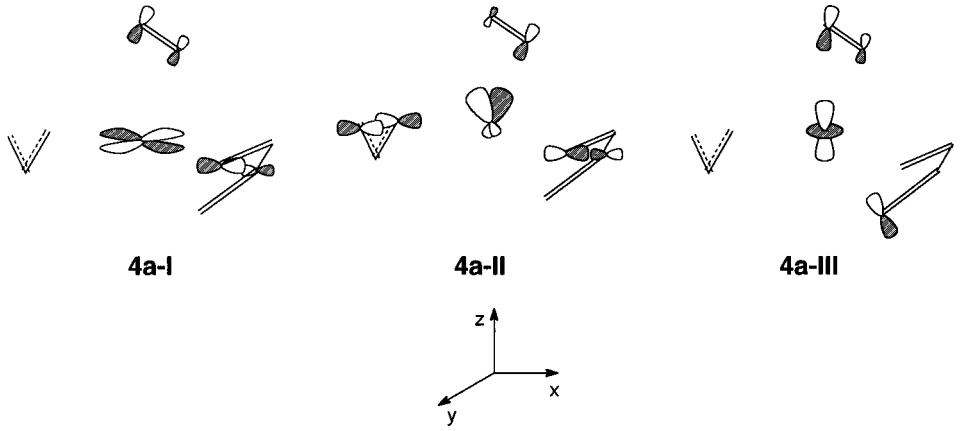

Figure 9.

Table 2. Calculated Energy Profile for the π-Allyl Insertion into the Cationic $[Ni(C_3H_5)(C_4H_6)(C_2H_4)]^+$ System (kcal/mol)[a]

system	η^4-educt (**3a**/**4a**)	η^2-educt (**3b**/**4b**)	transn state (**3c**/**4c**)	product (**3d**/**4d**)
supine (**3a**−**d**)	37.7	34.1	11.3	49.3
prone (**4a**−**d**)	34.9	32.4	31.0	52.2

[a] The isolated reactants ($[Ni(\eta^3\text{-}C_3H_5)(\eta^2\text{-}C_2H_4)]^+$ and *s-cis*-C_4H_6) were chosen as reference points.

The out of plane bending angles[17] of about 26 and 24° for **3c** and **4c**, respectively, give a clear indication of the progress of the C−C bond generation which is associated with a change in hybridization for the adjacent carbon atoms at this stage of the reaction. The essentially sp^3-hybridized carbon atoms are beginning to move away from the nickel(II) coordination sphere, as already appeared for the $[Ni(C_3H_5)(C_4H_6)]^+$ system.

Although the simpler $[Ni(C_3H_5)(C_4H_6)]^+$ model gives essential insights into the mechanism as derived from the located transition state structures, a different picture between the supine and prone arrangements can only be found including ethylene. The coordinative interaction of ethylene with nickel(II) is very similar at each stage of the reaction, as indicated by the almost identical ligand geometry distortion, regardless of whether the allyl and butadiene are supine or prone oriented.

In free optimizations starting downhill from marginal distorted transition stage geometries (i.e. with both an elongated and shortened C−C distance toward the educts and products) it was proved that both transition states correspond to both the η^4-butadiene educts (**3a**, **4a**) and the products (**3d**, **4d**), respectively.

The energetics calculated by using the standard DZVP basis are reported in Table 2. The energy profile is summarized in Figure 10. We would expect a noticeable difference in energy from the above discussed geometrical and electronic aspects concerning the insertion reaction as discussed above especially for the transition states which resulted in quite different activation barriers for the supine and prone arrangements. Due to the inclusion of the ethylene ligand Tolman's 18−16 electron rule should be fulfilled, and in addition we expect more realistic reaction energies, compared to the experiment.

The formation of η^4-educts (**3a**, **4a**) is an exothermic process, which amounts to 37.7 and 34.9 kcal/mol, respectively. In contrast to the simpler $[Ni(C_3H_5)(C_4H_6)]^+$ model, the overall reaction is exothermic relative to both the isolated molecules by 49.3 kcal/mol (supine) and by 52.2 kcal/mol (prone) and the η^4-educts by 11.6 kcal/mol (supine) and by 17.3 kcal/mol (prone). The η^4- (**3a**, **4a**) and η^2- (**3b**, **4b**) educts are energetically similar, with the η^4-educts favored by about 3 kcal/mol. Thus, from the energetical point of view, both educts are eligible to be reactants for the insertion reaction, but on the other hand, the η^2-educts should be ruled out according to deductions from the principle of least structure variation. The most striking difference appears in the transition states. Whereas the supine mode achieves a similar activation barrier of 26.4 kcal/mol as for the $[Ni(C_3H_5)(C_4H_6)]^+$ model, the calculated insertion barrier amounts only 3.9 kcal/mol for the prone mode. The modest activation barrier found in this study stems from the fact that only a marginal change in the ligand coordination is required to form the transition state in the case of the prone orientation. Therefore, the prone orientation is strongly preferred in kinetic and in thermodynamic controls.

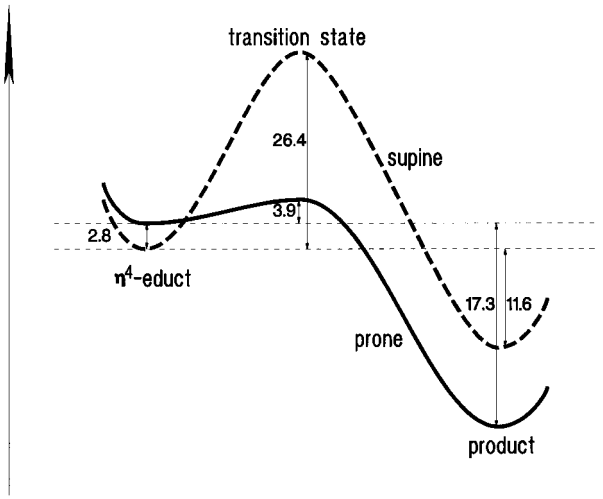

Figure 10. Reaction profile for the insertion of *cis*-butadiene into the *anti*-η^3-butenyl−nickel(II) bond for the cationic $[Ni(C_3H_5)(C_4H_6)(C_2H_4)]^+$ complex (in kcal/mol).

The calculated reaction energies are not influenced by using the larger TZVP basis. The activation barrier for supine remains the same, while a slightly higher value of about 6 kcal/mol was calculated for prone.

Conclusions

We have examined the insertion of *s-cis*-butadiene into the η^3-butenyl−nickel(II) bond attempting to show

Downloaded by CARLI CONSORTIUM on June 30, 2009
Published on August 6, 1996 on http://pubs.acs.org | doi: 10.1021/om960038d

that this process should be possible within the π-coordination of both reacting parts. The investigation was done on the $[Ni(C_3H_5)(C_4H_6)]^+$ and $[Ni(C_3H_5)(C_4H_6)(C_2H_4)]^+$ system, modeling the ligand-free cationic butenylnickel(II) complex.

No clear difference could be detected for both the main geometrical parameters and the reaction profile between the supine and prone coordination modes for the $[Ni(C_3H_5)(C_4H_6)]^+$ model. It was therefore necessary to incorporate the next double bond of the growing polymer chain in order to achieve an adequate description of the geometrical aspects, as well as for reliable energetics, clearly demonstrated by the $[Ni(C_3H_5)(C_4H_6)(C_2H_4)]^+$ model. A clear difference between the supine and prone orientations resulted for this system, especially in the transition states. The productlike supine transition state **3c** can be described as being tetragonal pyramidal, and the rather eductlike prone transition state **4c** can be described as being trigonal bipyramidal.

Due to the lack of coordinative saturation of the nickel(II) center in the $[Ni(C_3H_5)(C_4H_6)]^+$ system, the insertion was calculated to be endothermic with an insertion barrier of about 25 kcal/mol. A noticeable kinetic and thermodynamic preference for the prone instead of the supine orientation took place concerning the $[Ni(C_3H_5)(C_4H_6)(C_2H_4)]^+$ model. The insertion was determined to be exothermic by 11.6 kcal/mol (supine) and 17.3 kcal/mol (supine), with a barrier that amounts to 26.4 kcal/mol (supine) and 3.9 kcal/mol (prone).

Although the simpler $[Ni(C_3H_5)(C_4H_6)]^+$ model gives an essential insight into the mechanism, as derived from the transition state, it is the more realistic $[Ni(C_3H_5)(C_4H_6)(C_2H_4)]^+$ model which gives a different picture between the supine and prone arrangements. The transition states are characterized by a nearly complete change in hybridization of the affected carbon atoms of the newly formed C−C σ-bond from sp^2 to sp^3. As a consequence, these carbon atoms begin to move away from the nickel(II) coordination sphere, while the other moieties remain π-coordinated to nickel(II).

In further studies we will extend our investigations to the π-insertion of *cis*-butadiene into the *syn*/*anti*-η^3-butenyl−nickel(II) bond and the *trans*-butadiene π-insertion for monoligand nickel(II) complexes.

Acknowledgment. This work is supported by the Bundesministerium für Forschung und Technologie (BMFT). We acknowledge excellent service by the computer centers ZIB Berlin, URZ Magdeburg, and HLRZ Jülich.

Supporting Information Available: Tables of Cartesian coordinates of DFT optimized structures **1a**−**d**, **2a**−**d**, **3a**−**d**, and **4a**−**d** (16 pages). Ordering information is given on any current masthead page.

OM960038D

Downloaded by CARLI CONSORTIUM on June 30, 2009
Published on August 6, 1996 on http://pubs.acs.org | doi: 10.1021/om960038d